

STATIC AND EIGENVALUE ANALYSIS OF CRACKED TIMOSHENKO BEAM BY NEW MACRO ELEMENT CONTAIN ARBITRARY NUMBER OF CRACKS

Mohsen MEHRJOO

*Department of Civil Engineering, Islamic Azad University Hamedan Branch, Hamedan, Iran
mehrjoo_moh@yahoo.com*

Keywords: Static Analysis, Eigenvalue Analysis, Cracked Timoshenko Beam, New Macro Element

ABSTRACT

In this paper the finite element of beam element with arbitrary number of transverse cracks is derived for fatigue and fracture applications. The new element is one-dimensional with arbitrary number of embedded edge cracks in arbitrary position of beam element with any depth. The cracks are not physically modeled within the element, but instead, their influences on the local flexibility of the structure are considered by the modification of the element stiffness as a function of the cracks depth and cracks position. The derivations are based on a simplified computational model, where each crack is replaced by a corresponding linear rotational spring, connecting two adjacent elastic parts. The components of the stiffness matrix for the cracked element are derived using the superposition principle, compatibility relations, and Betti's theorem. The stiffness matrix for transversely cracked beam element is derived and all expressions are given in symbolic forms. Models using the presented stiffness matrix are shown to produce accurate results, although with significantly less computational effort than physical modeling of the crack in 2D finite element models.

INTRODUCTION

Cracks in structures present a serious threat to proper performance of structures. Most of failures of presently used structures are due to material fatigue. Experimental and computational studies have demonstrated that the presence of cracks leads to a change of the vibration properties of these structures (Cacciola et al, 2003, Dimarogonas, 1996 and Krawczuk et al, 2000). Because, due to the crack presence, the structures miss their original stiffness. Monitoring the change of these properties over time represents a widely used nondestructive method of evaluating the severity of the damage and computing the remaining life of structure.

A detailed model of the crack and its surrounding can be properly obtained with an appropriate mesh of finite elements. From a computational viewpoint, the finite element method represents a standard approach to simulate how cracked structures treat under external loading. The majority of these methods introduce the crack by physically modeling the separation of the two crack faces. A major disadvantage of these methods is that they necessitate the allocation of significant computational efforts in order to accurately model the stress singularity at the crack tip. However, such an approach is unsuitable for inverse problems where a model suitable for crack location and depth modification is required when searching for a potential crack.

For some applications, the global response of a cracked structure is of interest, while the local behavior of the material in the vicinity of the crack tip can be disregarded. In such cases there is a need for simulating the crack presence without actually modeling the crack. In this paper we present such an approach applied to a one-dimensional finite element that has arbitrary number of embedded cracks in different

positions of element with different depths. The conceptual illustration of the presented element with modified stiffness matrix is presented in Figure 1. The presence of the cracks is introduced by changing the stiffness matrix of the element. This type of element can be used in structural applications to compute response of a cracked structure under loading. Also it can be used for eigenvalue analysis of structures.

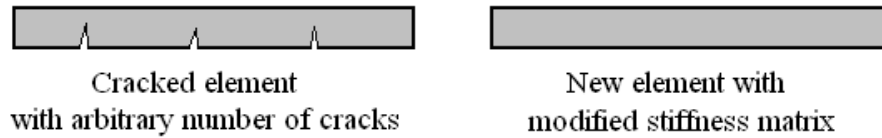


Figure 1. Conceptual illustration for the new finite element: the cracks are removed from the physical model and the stiffness matrix is modified

In this way simplified model, given by Ostachowicz and Krawczuk (1991) are implemented, where the crack is replaced by a rotational linear spring connecting the uncracked parts of the structure that are modeled as elastic elements. Ostachowicz and Krawczuk introduced the definition for rotational linear spring stiffness for a cracked rectangular cross-section.

Therefore, in order to improve the efficiency of the existing computational model for transversely cracked beam elements, the paper considers the derivation of a new beam finite element and presents the derivation of a stiffness matrix for transversely cracked beams subjected to transverse loads.

MACRO ELEMENT WITH ARBITRARY NUMBER OF TRANSVERSE CRACKS

THE EQUIVALENT STIFFNESS FOR OPEN SINGLE- SIDED CRACK

Open single sided crack is illustrated in Figure 2. Under service conditions cracks of this type occur under fluctuating loads.

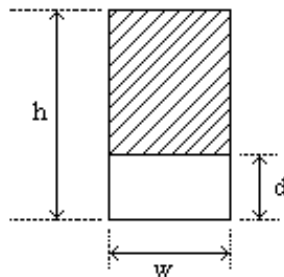


Figure 2. Single-sided crack (dimensions)

The equivalent rotational spring stiffness at the through-the-thickness single- sided crack location is presented as follows (Ostachowicz and Krawczuk, 1991):

$$K = \frac{Ewh^2}{72\pi \times f(\eta)} \quad (1)$$

where

$$\eta = \frac{d}{h} \quad (2)$$

$$f(\eta) = 0.6384(\eta)^2 - 1.035(\eta)^3 + 3.7201(\eta)^4 - 5.1773(\eta)^5 + 7.553(\eta)^6 - 7.332(\eta)^7 + 2.4909(\eta)^8 \quad (3)$$

Where, d is crack depth, w is beam width or thickness, h is its depth of beam and E is modulus of elasticity.

DERIVATION OF STIFFNESS MATRIX

The derivation of the new finite element is based on a mathematical model for a beam element with arbitrary number of transverse cracks as given by Ostachowicz and Krawczuk (1991). The cracks are introduced as a rotational linear spring connecting two elastic uncracked parts (Figure 3) and is defined by its location (i.e. the distance αL from the left end that $0 \leq \alpha \leq 1$) and depth d that is modeled with rotational spring stiffness denoted with S that depends on w, d, h and E .

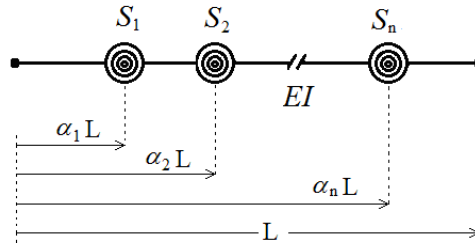


Figure 3. Beam element with arbitrary number of transverse cracks

The stiffness matrix in general represents the relationship between the forces (and moments) and the corresponding displacements, i.e. transverse translations and rotations at the ends of the beam element. The basic idea is the superposition principle.

Considering only transverse displacements, and with disregarding axial deformation in beam elements, the finite element has 4 degrees of freedom. This consequently means that 2 degrees of freedom must be simultaneously removed. Consequently, 4 degrees of freedom have to be considered to obtain all the required coefficients of the stiffness matrix. Nodal degree of freedom consist of lateral translation v_1 and v_2 and rotations θ_{z1} and θ_{z2} about the z axis (normal to paper).

The element stiffness matrix K can be constructed column by column. To obtain terms in a column we must solve statically indeterminate beam problem. For derivation of terms in a column in stiffness matrix, d.o.f.(degree of freedom) of element corresponding to that d.o.f. moved unit value in direction of that d.o.f. and another degree of freedoms is constrained. Nodal forces and moment that must be applied to sustain a deformation state in which that d.o.f. has unit value and all other d.o.f. are zero, are labeled according to their position in K and with proper algebraic sign: positive directions are upward for translation and force and counterclockwise for rotation and moment(Figure 4).

This results in a statically indeterminate beam problem, which is solved using the superposition principle, compatibility relations and Betti's theorem [5] in this paper. In this way, simple formulation of translation and rotation at the end of the cantilever beam under concentrated transverse load (P) and concentrated moment (M) is used. Relations of deflection (Δ) and slope of deflection (θ) caused by moment at the end of the cantilever beam under concentrated loading applied to end of beam are as follows:

$$\Delta = \frac{PL^3}{3EI} \quad (4)$$

$$\theta = \frac{PL^2}{2EI} \quad (5)$$

in which, P is concentrated transverse load, L is beam length, I is the moment inertia and E is modulus of elasticity. Also, relations of deflection (Δ) and slope of deflection (θ) caused by moment at the end of the cantilever beam under concentrated moment applied to end of beam are as follows:

$$\Delta = \frac{ML^2}{2EI} \quad (6)$$

$$\theta = \frac{ML}{EI} \quad (7)$$

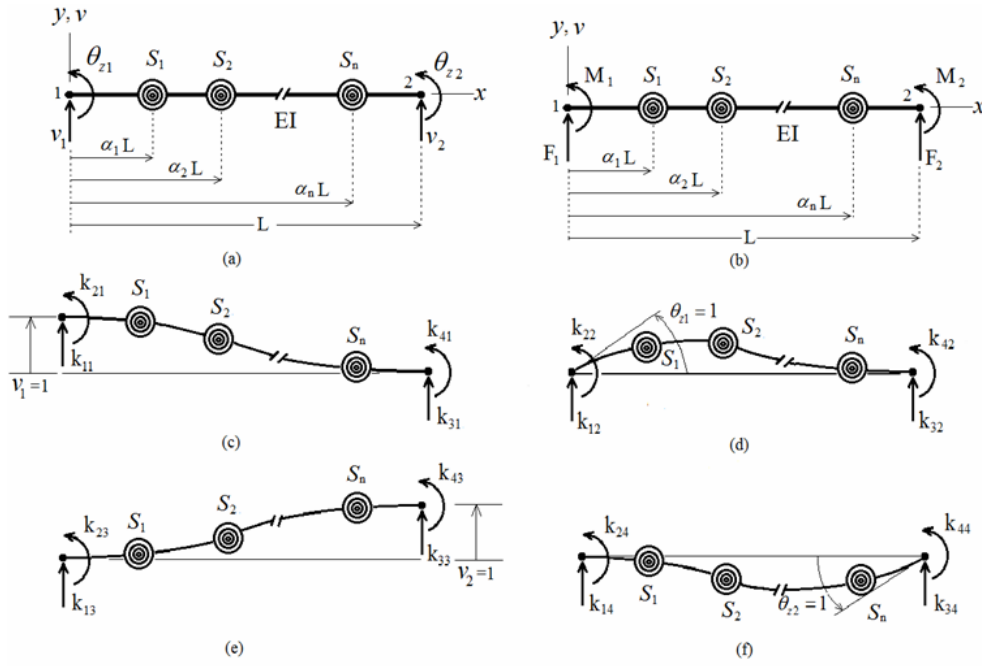


Figure 4. (a) Beam element and its nodal d.o.f. (b) Nodal load associated with d.o.f. (c-f) Deflected shapes associated with activation of each d.o.f. in turn. Nodal loads are labeled according to their position in K

in which, M is concentrated moment, L is beam length, I is the moment inertia and E is modulus of elasticity. Also, deflection (Δ) caused by shear force at the end of the cantilever beam under concentrated transverse loading applied to end of beam is as follows:

$$\Delta = \frac{PL}{GA_s} \quad (8)$$

in which, (A_s) is the shear cross section, P is the concentrated transverse load and G is the shear modulus of elasticity.

DERIVATION OF FIRST COLUMN OF STIFFNESS MATRIX FOR SAMPLE

In order to derive the first column of K , the left support is moved as the unit value in the direction of the first DOF, whereas other DOFs are constrained (Figure 5(a)). In this state, forces and moments in nodal DOF are corresponded to first column of matrix. In this stage, we use superposition principle, and apply k_{11} and k_{21} separately and satisfy compatibility equations (Figure 5(b) and (c)).

Δ_1 and θ_1 in Figure 5(b) are calculated using Equations (4)–(8) as follows:

$$\Delta_1 = \frac{k_{11}L^3}{3EI} + \frac{k_{11} \times \alpha_1 L}{S_1} \times \alpha_1 L + \frac{k_{11} \times \alpha_2 L}{S_2} \times \alpha_2 L + \dots + \frac{k_{11} \times \alpha_n L}{S_n} \times \alpha_n L + \frac{k_{11}L}{GA_s}$$

$$\theta_1 = \frac{-k_{11}L^2}{2EI} - \frac{k_{11} \times \alpha_1 L}{S_1} - \frac{k_{11} \times \alpha_2 L}{S_2} - \dots - \frac{k_{11} \times \alpha_n L}{S_n}$$

Δ_2 and θ_2 in Figure 5(c) are calculated using Equations (4)–(8) as follows:

$$\Delta_2 = \frac{-k_{21}L^2}{2EI} - \frac{k_{21} \times \alpha_1 L}{S_1} - \frac{k_{21} \times \alpha_2 L}{S_2} - \dots - \frac{k_{21} \times \alpha_n L}{S_n}$$

$$\theta_2 = \frac{k_{21}L}{EI} + \frac{k_{21}}{S_1} + \frac{k_{21}}{S_2} + \dots + \frac{k_{21}}{S_n}$$



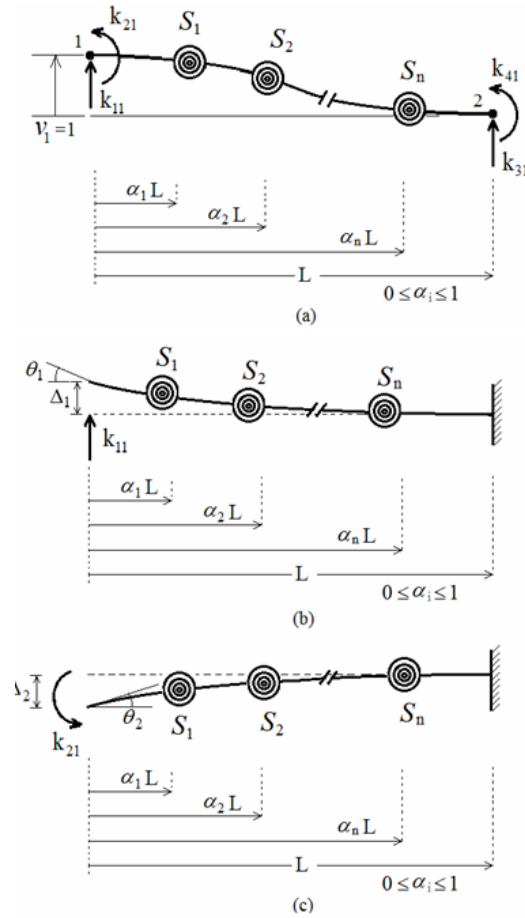


Figure 5. (a) activation of first d.o.f. unit value .Nodal loads are labeled according to first column in K (b-c) applying nodal loads separately.

With writing compatibility equations of rotation, we can write as follows:

$$\begin{aligned}
 \theta_1 + \theta_2 &= 0 \Rightarrow \\
 k_{21} &= \frac{S_1 S_2 \dots S_n L^2 + 2EIS_2 S_3 \dots S_n \alpha_1 L + 2EIS_1 S_3 S_4 \dots S_n \alpha_2 L + \dots + 2EIS_1 S_2 S_3 \dots S_{n-1} \alpha_n L}{2S_1 S_2 \dots S_n L + 2EIS_2 S_3 \dots S_n + 2EIS_1 S_3 S_4 \dots S_n + \dots + 2EIS_1 S_2 \dots S_{n-1}} k_{11} \\
 \Rightarrow A &= \frac{S_1 S_2 \dots S_n L^2 + 2EIS_2 S_3 \dots S_n \alpha_1 L + 2EIS_1 S_3 S_4 \dots S_n \alpha_2 L + \dots + 2EIS_1 S_2 S_3 \dots S_{n-1} \alpha_n L}{2S_1 S_2 \dots S_n L + 2EIS_2 S_3 \dots S_n + 2EIS_1 S_3 S_4 \dots S_n + \dots + 2EIS_1 S_2 \dots S_{n-1}} \\
 \Rightarrow k_{21} &= A k_{11} \\
 \Delta_1 + \Delta_2 = 1 &\Rightarrow k_{11} \left(\frac{L^3}{3EI} + \frac{\alpha_1^2 L^2}{S_1} + \frac{\alpha_2^2 L^2}{S_2} + \dots + \frac{\alpha_n^2 L^2}{S_n} + \frac{L}{GA_S} \right) - \frac{k_{21} L^2}{2EI} - \frac{k_{21} \alpha_1 L}{S_1} - \frac{k_{21} \alpha_2 L}{S_2} - \dots - \frac{k_{21} \alpha_n L}{S_n} = 1 \\
 k_{21} &= A k_{11} \Rightarrow \\
 k_{11} \left[\frac{L^3}{3EI} + \frac{\alpha_1^2 L^2}{S_1} + \frac{\alpha_2^2 L^2}{S_2} + \dots + \frac{\alpha_n^2 L^2}{S_n} + \frac{L}{GA_S} - \frac{AL^2}{2EI} - \frac{A\alpha_1 L}{S_1} - \frac{A\alpha_2 L}{S_2} - \dots - \frac{A\alpha_n L}{S_n} \right] &= 1 \Rightarrow \\
 B = \frac{L^3}{3EI} + \frac{\alpha_1^2 L^2}{S_1} + \frac{\alpha_2^2 L^2}{S_2} + \dots + \frac{\alpha_n^2 L^2}{S_n} + \frac{L}{GA_S} - \frac{AL^2}{2EI} - \frac{A\alpha_1 L}{S_1} - \frac{A\alpha_2 L}{S_2} - \dots - \frac{A\alpha_n L}{S_n} &= 1
 \end{aligned}$$

$$k_{11} = \frac{1}{B} \quad (9)$$

$$k_{21} = \frac{A}{B} \quad (10)$$

$$\sum F_y = 0 \Rightarrow k_{31} = -\frac{1}{B} \quad (11)$$

$$\sum M = 0 \Rightarrow k_{41} = \frac{L-A}{B} \quad (12)$$

DERIVATION OF OTHER COLUMNS OF THE STIFFNESS MATRIX

The remaining columns of K may be simply derived using the same procedure as the First column. Consequently, the closed-form of the stiffness matrix may be given as follows:

$$K = \begin{bmatrix} \frac{1}{B} & \frac{A}{B} & -\frac{1}{B} & \frac{L-A}{B} \\ \frac{A}{B} & C\frac{A}{B} & -\frac{A}{B} & \frac{A(L-C)}{B} \\ \frac{B}{-1} & \frac{B}{-A} & \frac{B}{1} & \frac{B}{A-L} \\ \frac{B}{L-A} & \frac{B}{A(L-C)} & \frac{B}{A-L} & \frac{B}{L^2 - 2AL + AC} \end{bmatrix} \quad (13)$$

$$A = \frac{S_1 S_2 \dots S_n L^2 + 2EIS_2 S_3 \dots S_n \alpha_1 L + 2EIS_1 S_3 S_4 \dots S_n \alpha_2 L + \dots + 2EIS_1 S_2 S_3 \dots S_{n-1} \alpha_n L}{2S_1 S_2 \dots S_n L + 2EIS_2 S_3 \dots S_n + 2EIS_1 S_3 S_4 \dots S_n + \dots + 2EIS_1 S_2 \dots S_{n-1}} \quad (14)$$

$$B = \frac{L^3}{3EI} + \frac{\alpha_1^2 L^2}{S_1} + \frac{\alpha_2^2 L^2}{S_2} + \dots + \frac{\alpha_n^2 L^2}{S_n} + \frac{L}{GA_S} - \frac{AL^2}{2EI} - \frac{A\alpha_1 L}{S_1} - \frac{A\alpha_2 L}{S_2} - \dots - \frac{A\alpha_n L}{S_n} \quad (15)$$

C =

$$\frac{2GA_S S_1 S_2 \dots S_n L^3 + 6EIGA_S S_2 S_3 \dots S_n \alpha_1^2 L^2 + 6EIGA_S S_1 S_3 S_4 \dots S_n \alpha_2^2 L^2 + \dots + 6EIGA_S S_1 S_2 S_3 \dots S_{n-1} \alpha_n^2 L^2 + 6EIS_1 S_2 \dots S_n L}{3GA_S S_1 S_2 \dots S_n L^2 + 6GA_S EIS_2 S_3 \dots S_n \alpha_1 L + 6GA_S EIS_1 S_3 S_4 \dots S_n \alpha_2 L + \dots + 6GA_S EIS_1 S_2 S_3 \dots S_{n-1} \alpha_n L} \quad (16)$$

MASS MATRIX OF CRACKED ELEMENT

Since it was stated by Krawczuk et al (2000) in dynamic analysis of beam like structures the inertia matrix for non-cracked structures can be conveniently used for cracked elements, for mass matrix of cracked element we can use of mass matrix of sound element.

VERIFICATION OF THE NEW CRACKED MACRO ELEMENT BY 2D FINITE ELEMENT RESULTS

The proposed cracked macro element is verified considering various loadings, and boundary conditions of cracked beams. Results from a 2D finite element model are employed to confirm the accuracy of the present cracked beam element. All the cracked beam models are made of a material with the following properties: the modulus of elasticity $E = 200$ GPa, the material mass density $= 7800$ kg/m³, and the Poisson ratio $\nu = 0.3$. The considered geometric data are: the beam length $L=4$ m, the cross-section of the beam is a rectangle with depth $h = 200$ mm and width $w = 100$ mm. Three single-sided transverse cracks with depths $d = 60$ mm, $d=100$ mm and $d=80$ mm are located at distances 1.25m, 1.5 m and 1.75 m from the left support, respectively.



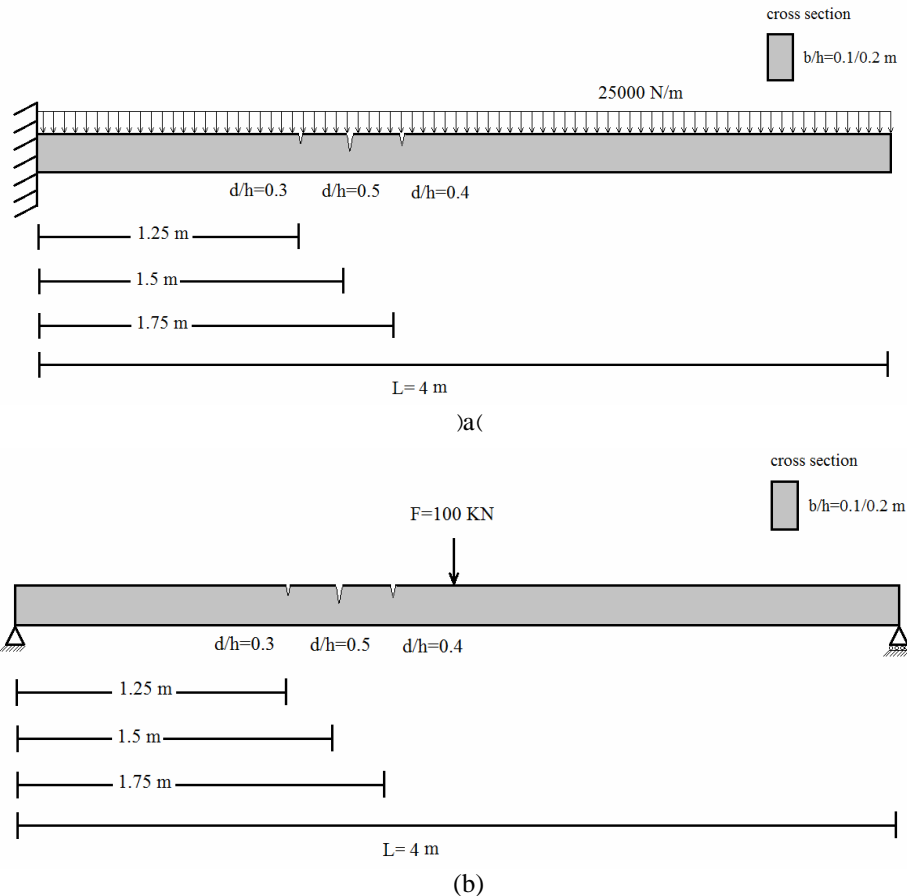


Figure 6. The loadings and boundary conditions for the static and eigenvalue analysis of the cracked beam.

CONVERGENCE TEST OF FINITE ELEMENT MODELS

It should be noted that blind application of finite element model to solve eigenvalue problem for finding the natural frequencies, without considering the assumptions under which the crack models are derived, may lead to remarkable errors. For the finite element models of the present research, the beam is discretized by four-node isoparametric plane-stress elements. In this element, drilling DOFs are employed to improve the behaviour of the element in bending vibration problems (Zienkiewicz and Taylor, 2000). In each example, the mesh density has been examined by the convergence test (Zienkiewicz and Taylor, 2000) for cracked and uncracked beams. The results of convergence test determine the suitable and enough fine meshes whose natural frequencies are almost identical to exact natural frequencies available for uncracked beams (Timoshenko et al, 1974). As a result, in the next sections, the most appropriate finite element meshes have been chosen based on the results of corresponding convergence tests in each example. For these examples, the 2D finite element model consists of 8000 four-node quadrilateral elements and the new finite element model consists of four new beam elements.

STATIC ANALYSIS

In this section, two different combinations of loadings and boundary conditions are presented to validate the proposed cracked macro element in static analysis. In the first combination, a cantilever beam was considered (Figure 6(a)). The beam is under a transverse uniformly distributed loading of 25 kN/m throughout the beam. In the second combination, a simply supported beam with a transverse concentrated load of 100 kN at the middle point of the beam is studied (Figure 6(b)). Both combinations are modeled using four new finite elements with the length of 1 m (Figure 7). After deriving stiffness matrix for all elements, stiffness matrixes were assembled and then with using below relation displacements and rotations were derived:

$$D = K^{-1} \times F \quad (17)$$

Where D is displacement vector and K is the stiffness matrix and F is load vector. The transverse displacements and rotations at points A, B, C, D and E are obtained using the new element and the 2D finite element analyses (Section 3.1). Table 1 gives the comparison between the results of two methods. As may be seen from Table 1, the results of two methods present good agreement.

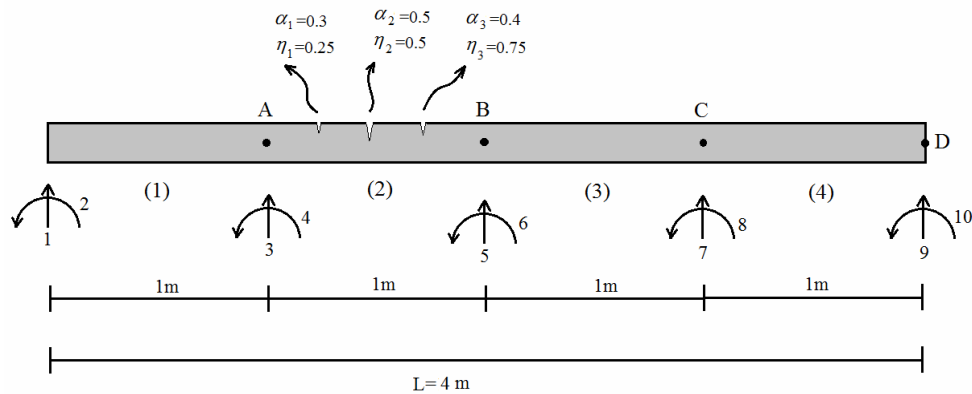


Figure 7. The cracked beam modeled by four cracked finite elements (10 DOFs).

EIGENVALUE ANALYSIS

In this section, two boundary conditions of Section 3.2 are considered to verify the proposed cracked macro element in eigenvalue analysis. Since from numerical point of view the form of the inertia matrix does not affect natural frequencies (Krawczuk et al, 2000), in eigenvalue solution is used from mass matrix of uncracked beam element that can be found in all standard books about finite elements. Also with using below equation modal analysis was performed, and the natural frequencies for the first three vibration modes were computed:

$$\left| K - \omega^2 M \right| = 0 \quad (18)$$

Where K is the stiffness matrix and M is the mass matrix and ω is frequency of structure.

In addition, the same meshes of Section 3.2 are used in these analyses to compute the natural frequencies for the first three vibration modes of each boundary condition (see Table 2). As may be seen from Table 2, the results of two methods present good agreement.

Table 1. Comparison of transverse displacements and rotations obtained from new cracked macro element and 2D finite element for considered examples.

Boundary Conditions	Element	Point A		Point B		Point C		Point D		Point E	
		$u(m)$	$\theta(rad)$								
Cantilever beam	Quadrilateral four-node element	0.00	0.00	0.0064	0.0116	0.0254	0.0258	0.0525	0.0280	0.0808	0.0283
	New cracked beam element	0.00	0.00	0.0063	0.0116	0.0247	0.0245	0.0505	0.0267	0.0774	0.0270
Simply-supported beam	Quadrilateral four-node element	0.00	0.0126	0.0120	0.0108	0.0166	0.0032	0.0102	0.0089	0.00	0.0108
	New cracked beam element	0.00	0.0118	0.0111	0.0099	0.0154	0.0027	0.0096	0.0083	0.00	0.0102



Table 2. Comparison of natural frequencies (HZ) obtained from new cracked macro element and 2D finite element for considered examples.

Boundary Conditions	Element	Mode 1	Mode 2	Mode 3
Cantilever beam	Quadrilateral four-node element	8.81	54.90	157.31
	New cracked beam element	9.01	56.77	167.52
Simply-supported beam	Quadrilateral four-node element	22.5	102.62	228.40
	New cracked beam element	23.36	106.57	246.78

CONCLUSIONS

A new macro element is derived for the analysis of Timoshenko beams with transverse cracks. For driving stiffness matrix for cracked beam element with arbitrary number of cracks, cracks were modeled with torsional spring and for their rotational stiffness was used of relation presented by Ostachowicz and Krawczuk for open cracks and influence of the flexibility of the element due to the cracks presence was derived using the superposition principle, compatibility relations, and Betti's theorem. The accuracy of the new macro element was verified by comparing the displacements and rotations and frequency response of a beam with three edge crack through via two example. In both examples the beam was modeled using new macro element account for the crack presence, and also by physically modeling the cracks in 2D finite element meshing. The new macro element produced excellent results when compared with those from the physical crack model. The proposed model has two limitations. The first limitation of the presented finite elements is the absence of information about stress distribution in the vicinity of the cracks. Therefore, in situations where this information is essential (for the crack propagation analysis) this model cannot be applied. However, from the pure inverse identification point of view, this limitation is not essential, as the non-propagation of cracks is assumed during the analysis. The second limitation of the presented finite elements is the analytical formulation of the cracked element takes into account the reduction in stiffness only for the case of open cracks. The stiffness change of an element with closed cracks is not analyzed in this paper.

REFERENCES

- Cacciola P, Impollonia N and Muscolino G (2003) Crack detection and location in a damaged beam vibrating under white noise, *Computer & Structures*, 81:1773–82
- Dimarogonas AD (1996) Vibration of cracked structures: a state of the art review, *Engineering Fracture Mechanics*, 55: 831–57
- Krawczuk M, Zak A and Ostachowicz W (2000) Elastic beam finite element with a transverse elasto-plastic crack, *Finite Elements in Analysis and Design*, 34: 61–73
- Owolabi GM, Swanidas ASJ and Seshadri R (2003) Crack detection in beams using changes in frequencies and amplitudes of frequency response function, *Journal of Sound and Vibration*, 265:1–22
- Ostachowicz WM and Krawczuk M (1991) Analysis of the effect of cracks on the natural frequencies of a cantilever beam, *Journal of Sound and Vibration*, 150 (2): 191–201
- Timoshenko S, Young DH and Weaver W (1974) *Vibration problems in engineering*, New York, Wiley
- Wang CK (1983) *Intermediate structural analysis*, Singapore: McGraw-Hill
- Zienkiewicz OC and Taylor RL (2000) *the finite element method*, Oxford: Butterworth and Heinmann